

A First Principles Density-Functional Calculation of the Electronic and Vibrational Structure of the Key Melanin Monomers*

B. J. Powell,^{1,†} T. Baruah,^{2,3} N. Bernstein,² K. Brake,¹ Ross H. McKenzie,¹ P. Meredith¹ and M. R. Pederson²

¹*Department of Physics, University of Queensland, Brisbane, Queensland 4072, Australia*

²*Center for Computational Materials Science, U.S. Naval Research Laboratory, Washington, D.C. 20375, USA and*

³*Department of Physics, Georgetown University, Washington, D.C. 20057, USA*

We report first principles density functional calculations for hydroquinone (HQ), indolequinone (IQ) and semiquinone (SQ). These molecules are believed to be the basic building blocks of the eumelanins, a class of bio-macromolecules with important biological functions (including photo-protection) and with potential for certain bioengineering applications. We have used the Δ SCF (difference of self consistent fields) method to study the energy gap between the highest occupied molecular orbital (HOMO) and the lowest unoccupied molecular orbital (LUMO), Δ_{HL} . We show that Δ_{HL} is similar in IQ and SQ but approximately twice as large in HQ. This may have important implications for our understanding of the observed broad band optical absorption of the eumelanins. The possibility of using this difference in Δ_{HL} to molecularly engineer the electronic properties of eumelanins is discussed. We calculate the infrared and Raman spectra of the three redox forms from first principles. Each of the molecules have significantly different infrared and Raman signatures, and so these spectra could be used *in situ* to non-destructively identify the monomeric content of macromolecules. It is hoped that this may be a helpful analytical tool in determining the structure of eumelanin macromolecules and hence in helping to determine the structure-property-function relationships that control the behaviour of the eumelanins.

PACS numbers: 87.15.-v, 82.35.Cd, 87.64.Je

I. INTRODUCTION

The melanins are an important class of pigmentary macromolecule found throughout the biosphere [1]. Pheomelanin (a cysteinyl-dopa derivative) and eumelanin (formed from 5,6-dihydroxyindolequinone and other indolequinones) are the predominant forms in humans, and act as the primary photoprotectant in our skin and eyes. Consistent with this role, all melanins show broad band monotonic absorption in the UV and visible in the range 1.5 to 5 eV [2]. In contrast, other biomolecules such as proteins and nucleic acids show only well defined absorption peaks around 280 nm (4.5 eV) and little absorption below that [3]. They are also efficient free radical scavengers and antioxidants [1]. In direct contradiction with these photoprotective properties, both pheomelanin and eumelanin are implicated in the development of melanoma skin cancer [4]. For this reason, the photophysics, photochemistry and photobiology of melanins are subjects of intense scientific interest.

Despite work over several decades (with respect to eumelanin in particular), the more general structure-property-function relationships that control the behaviour of these important bio-macromolecules are still poorly understood [5]. The melanins are difficult

molecules to study: they are chemically and photochemically stable, and are virtually insoluble in most common solvents. It is fairly well accepted that eumelanins are macromolecules of the various redox forms of 5,6-dihydroxyindolequinone (DHI or HQ) and 5,6-dihydroxyindole 2-carboxylic acid (DHICA) [1, 6]. However, major questions still remain concerning their basic structural unit [7]. Two opposing schools of thought exist: i) that eumelanins are composed of highly cross-linked extended hetero-polymers based upon the Raper-Mason scheme [1], and ii) that eumelanins are actually composed of much smaller oligomers condensed into 4 or 5 oligomer nano-aggregates [8]. Clearly, this is a fundamental issue, and is the starting point for the construction of consistent structure-property-function relationships.

The answer to this question also has profound implications for our understanding of the condensed phase properties of melanins. In 1960 Longuet-Higgins [9], in a landmark paper, proposed that many of the physical properties of melanins could be understood if they were semiconductors. This proposition was lent further support by Pullman and Pullman [10] in 1964 who applied molecular orbital theory in its simplest form (the Hückel approximation) to 5,6-dihydroxyindole and one particular dimer type. This theoretical work was followed in 1974 by the experimental observations of McGinness, Corry and Proctor who demonstrated that a pellet of melanin could be made to behave as an amorphous electrical switch [11]. They postulated that these materials may indeed be disordered organic semiconductors consistent with the Longuet-Higgins theory, and the newly developed models of amorphous inorganic semiconductors [12]. Several

*This work relates to Department of the Navy Grants N00014-03-1-4115, N00014-02-1-1046 and N00014-03-1-4116 issued by the Office of Naval Research International field office. The United States Government has a royalty-free license throughout the world in all copyrightable material contained herein.

[†]Electronic address: powell@physics.uq.edu.au

studies since have also claimed to show that melanins in the condensed solid-state are semiconductors [13, 14]. However, it is by no means certain that the conductivity reported in any of these experimental studies is electronic in nature. A clear idea of the basic structural unit is critical to developing a consistent model for condensed phase charge transport in such disordered organic systems. It is also important in the context of “molecularly engineering” melanins to have the ability to create or enhance functionality in high technology applications such as biosensors and bio-mimetic photovoltaics [15, 16].

It is well known that disorder plays a crucial role in determining the charge transport properties of amorphous inorganic semiconductors. In addition to the usual impurity related disorder, organic semiconductors (of which eumelanin may well be an exotic example), present several different sources of disorder associated with structural heterogeneity. For example, if one considers either the hetero-polymer or oligomer models, there are many different ways of constructing a eumelanin macromolecule based upon the monomer sequences, cross-linking positions or tautomer combinations. These possibilities have been studied theoretically for DHI-based macromolecules using a number of quantum chemical techniques. Notably, Galvao and Caldas [17, 18, 19] used the Hückel approximation to construct model homopolymers. Intriguingly, they found that many of the important “semiconductor related properties of eumelanin” stabilise at a relatively small number of monomer units - five or six in fact. Although they did not consider inter-chain effects, and essentially treated chain terminations as end defects, their work was the first indication that large, extended hetero-polymeric structures are not required to explain the physical properties of melanins. Bolivar-Marinez *et al.* [20] and Bochenek and Gudowska-Nowak [21] have used the intermediate neglect of differential overlap (INDO) and other semi-empirical methods to perform similar calculations for oligomers, whilst other authors have utilised the power of density functional theory to perform first principles calculations [5, 22] on single monomers or dimers.

Il'ichev and Simon [22] considered the hydroquinone, (HQ) and indolequinone (IQ) forms (see figure 1), and determined them to be the most stable and hence the most likely forms of the monomers. However, several pulse radiolysis studies [23, 24, 25, 26, 27, 28] have indicated the presence of the semiquinone (SQ - also shown in figure 1), a tautomer of IQ, and so we also consider SQ here.

Motivated by the remarkable optical absorption characteristics of eumelanins, many of these authors have focused on simulating the absorption spectra of HQ, IQ, SQ and related small oligomers [5, 20, 22]. However, knowledge of the electronic states around the highest occupied molecular orbital (HOMO) and lowest unoccupied molecular orbital (LUMO) levels is only part of the story. A great deal of information is also contained within the vibrational and rotational structure of the molecules. In particular, the IR and Raman spectra may

be useful analytical tools. This has proven to be the case in other biomolecules [3]. They can be used to confirm the accuracy of the first principles predictions by direct comparison with experimental evidence, and also to provide useful insight into local environment phenomena such as solvent-solute interactions. Furthermore, our IR and Raman spectra calculations have the advantage of coming from first principles calculations and not the semi-empirical methods often employed to calculate the absorption spectra.

In this paper we present a full density functional theory (DFT) analysis of the electronic, vibrational and rotational structure of the indolequinone (IQ), the semiquinone (SQ) and the hydroquinone (HQ). Our study is a considerable extension of previously published work since we: i) present calculated IR and Raman spectra for the first time, and ii) use the difference of self consistent fields (Δ SCF) approach to gain a more accurate understanding of the LUMO level. We find that the electronic properties of the molecules are highly dependent upon the redox form. Hence, we can say that oligomers or hetero-polymers consisting of one or more redox forms will have large variations in the local chemical potential, or, in the language of the tight binding model, strongly random site energies and possibly also random hopping integrals. This is to say that such hetero-structures will be highly disordered.

Our work is motivated by the desire to understand the implications of the redox form of the basic structural unit of eumelanins on the materials bulk properties. Such knowledge is a key starting point in any attempts to understand charge transport in and the optical properties of these disordered heterogeneous organic conductors. It also has profound implications in unravelling the mysteries of melanin biological functionality, and attempts to molecularly engineer melanin-like molecules for technological applications. These preliminary theoretical calculations are part of an ongoing quantum chemical, experimental solid-state and spectroscopic program aimed at gaining a more complete understanding of melanin structure-property-function relationships.

II. CALCULATION DETAILS

The chemical and electronic structures and the Raman and IR spectra were found from first principles DFT calculations. We have performed our calculations using the Naval Research Laboratory Molecular Orbital Library (NRLMOL) [29, 30, 31, 32, 33, 34, 35]. NRLMOL performs massively parallel electronic structure calculation using gaussian orbital methods. In particular, for a discussion of the calculation of the Raman and IR spectra see Refs. [33, 34, 35]. Throughout we have used the Perdew, Burke and Ernzerhof (PBE) [36] exchange correlation functional, which is a generalised gradient approximation (GGA) containing no parameters. For each molecule we have fully relaxed the geometry with no sym-

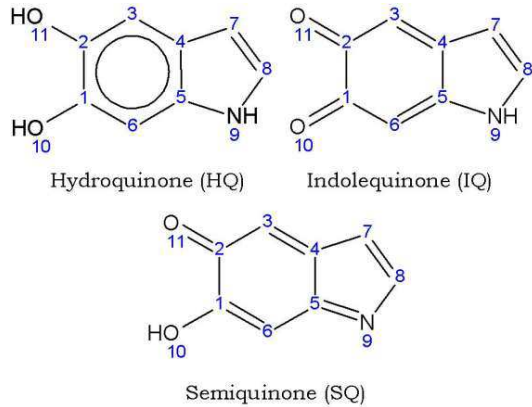


FIG. 1: Schematic representation of the 5,6-dihydroxyindolequinone (DHI) redox forms: hydroquinone (HQ) and the tautomers indolequinone (IQ) and semiquinone (SQ). The numbers correspond to those used in table II.

TABLE I: The total energy (in eV) of the two lowest energy tautomers of indolequinone (IQ); semiquinone (SQ) and 2-semiquinone (2-SQ) which is simply SQ with the hydrogen atom bonded to O11 rather than O10 (c.f. figure 1). The energies are quoted relative to the energy of IQ. In each case we fully relaxed the geometries as shown in figures 3 and 4. Our results for HQ, IQ and SQ are consistent with the calculations of Il'ichev and Simon [22]. The concentrations at 300 K are in direct contradiction to the experimental evidence [23, 24, 25, 26, 27, 28] that SQ is one of the building blocks of eumelanin.

Molecule	Name in Ref. 22	Energy (eV)	Concentration at $T = 300$ K
IQ	3a	0	87%
2-SQ	3d	0.05	13%
SQ	3c	0.19	< 0.1%

metry constraints.

III. RESULTS AND DISCUSSION

To benchmark our calculations we report the bond lengths and bond angles of HQ, IQ and SQ found in our calculations in table II. Our results are in good agreement with those calculated by Bolivar-Marinez *et al.* [20] and Stark *et al.* [5]. All three molecules are planar to within numerical accuracy (c.f., [5, 22]).

We find, in agreement with Il'ichev and Simon [22], that SQ is not the lowest energy tautomer of IQ (see table I). Indeed we find that at 300 K there should be less than 0.1% SQ. Although we should stress that this calculation is for a single molecule *in vacuo* it is, of course, in direct contradiction to the evidence [23, 24, 25, 26, 27, 28] that SQ is one of the building blocks of eumelanin. However, since SQ is widely thought to play an important role in eumelanin, we also consider it here.

As well as the ground state geometries shown in figures

TABLE II: The calculated bond lengths (in Å) and bond angles (in degrees) are found to be in good agreement with previous work [5, 20]. (Note that there is no experimental data to compare with.) The atom numbers correspond to those shown in figure 1.

	IQ	SQ	HQ
C1-C2	1.423	1.513	1.586
C2-C3	1.388	1.486	1.458
C3-C4	1.408	1.351	1.366
C4-C5	1.421	1.488	1.483
C5-C6	1.401	1.435	1.361
C6-C1	1.392	1.362	1.457
C4-C7	1.435	1.457	1.443
C7-C8	1.376	1.358	1.365
C8-N9	1.385	1.435	1.390
N9-C5	1.382	1.310	1.381
C1-O10	1.375	1.353	1.226
C2-O11	1.376	1.226	1.226
C1-C2-C3	120.69	117.88	118.32
C2-C3-C4	119.89	119.61	119.72
C3-C4-C5	118.45	120.78	121.03
C4-C5-C6	122.20	121.32	124.60
C5-C6-C1	118.18	118.79	118.34
C6-C1-C2	120.59	121.62	117.98
C3-C4-C7	134.47	134.88	132.73
C6-C5-N9	130.61	127.05	129.38
C4-C7-C8	107.08	105.05	107.23
C7-C8-N9	109.33	113.75	110.86
C8-N9-C5	109.32	105.23	109.65
N9-C5-C4	107.19	111.63	106.02
C5-C4-C7	107.08	104.34	106.24
O10-C1-C6	123.16	125.59	122.87
O10-C1-C2	116.24	112.79	119.15
O11-C2-C1	116.15	120.98	118.89
O11-C2-C3	123.16	121.14	122.79

2, 3 and 4 we also found stable geometries of HQ and SQ with the H-O-C bond angle increased by almost 180°. These alternative structures have significantly higher energies than the ground states. However, it is possible that the high energy structures may be stabilised by hydrogen bonding in a polar solvent. We therefore also considered the system SQ+6H₂O. We found that in this system the H-O-C bond is slightly larger than in SQ *in vacuo* (see figure 5). We also found a significant hydrogen bonded network around the H-O-C-C=O group which is dragged out of the plane of the molecule by interactions with the water molecules. This hydrogen bonding network is probably related to the fact that eumelanins are only soluble in polar solvents.

The Hückel model calculations of Galvao and Caldas [17] indicate that the HOMO-LUMO gap (Δ_{HL}) may be significantly larger in HQ than in either IQ or SQ. This has important implications in the context of understanding the basic eumelanin structural unit. Fundamentally, a combination of HQ and either IQ or SQ tautomers are present in an ensemble. Whether that ensemble be oligomeric or polymeric it can be expected to lead to an

apparent broadening of the absorption profile. In this situation, the key question is: how many monomers of HQ, IQ and SQ are required to create the broad band UV and visible absorbance over the range 1.5 to 5 eV that is macroscopically observable for eumelanins? The answer to this question may well allow us to assess the feasibility of the various structural models. Furthermore, when one considers the possibility that molecularly engineered forms of eumelanin may be useful as functional materials in electronic devices and sensors [15, 16], a critical design parameter is likely to be the “semiconductor” gap. It has previously been shown [18] that, at least within the Hückel approximation for homopolymers, the HOMO-LUMO gap of the monomer is closely related to the HOMO-LUMO gap of the infinite polymer, which, for the polymer model in the condensed solid state, corresponds to the semiconducting gap provided there is only weak coupling between polymers. Thus controlling the HOMO-LUMO gap of macromolecules may provide a route to controlling the semiconducting gap of eumelanins. This suggestion clearly needs further investigation, but controlling the HQ to IQ or SQ ratio may be a possible route to this form of property manipulation. An important first step to investigating either of these proposals is the calculation of the HOMO-LUMO gaps of the molecules by more reliable methods than Hückel theory.

In table III we compare the HOMO-LUMO gap found in our calculations with that found from the Hückel method [17]. For comparison with the Hückel calculations we need to estimate the hopping integral, β , in the Hückel Hamiltonian,

$$\hat{\mathcal{H}} = \sum_{i\sigma} (\alpha + \alpha' \delta_{i9}) \hat{c}_{i\sigma}^\dagger \hat{c}_{i\sigma} - \beta \sum_{\langle ij \rangle \sigma} \hat{c}_{i\sigma}^\dagger \hat{c}_{j\sigma}, \quad (1)$$

where α is the on-site energy, α' is the difference in the on-site energy between a nitrogen and a carbon atom (we take the labelling convention from figure 1 ensuring that the only nitrogen is in position $i = 9$), $\hat{c}_{i\sigma}^\dagger$ annihilates (creates) an electron with spin σ on site i and $\langle ij \rangle$ indicates that the sum is over nearest neighbours only. For hydrocarbons β is typically of order 2.5 eV [37]. Using this value of β we find that the HOMO-LUMO gaps for HQ, IQ and SQ found from the Hückel approximation are consistent with those found in our DFT calculations using the PBE functional. However, because DFT is a theory of the ground state, these calculations represent the energy gap between Kohn-Sham eigenvalues and not the true HOMO-LUMO gap of the molecules. This is known as the band gap problem [38]. Additionally, it is accepted that the PBE functional can significantly underestimate the HOMO-LUMO gap. Therefore we have also employed the Δ SCF method [38] to calculate Δ_{HL} . Our results clearly reproduce the trends seen in the time dependent density functional theory (TDDFT) calculations of Il'ichev and Simon [22] for IQ and SQ. The difference between the Δ SCF and TDDFT results for HQ probably indicates that the true value of Δ_{HL} is intermediate to

TABLE III: The HOMO-LUMO (highest occupied molecular orbital-lowest unoccupied molecular orbital) gap, Δ_{HL} , in eV. The HOMO-LUMO gap found from both the Δ SCF method and from a simple density functional calculation (both calculations use the PBE functional [36]) are compared with that found in the Hückel approximation (after [17], taking $\beta = 2.5$ eV which is the correct order of magnitude [37], c.f., (1)). It can be seen that the HOMO-LUMO gap of both the indolequinone (IQ) and the semiquinone (SQ) is significantly underestimated by both the Hückel approximation and the simple interpretation of the Kohn-Sham eigenvalues. However, these methods find a HOMO-LUMO gap for the hydroquinone (HQ) that is more consistent with the, more reliable, Δ SCF method. The results of the Δ SCF method indicate that the HOMO-LUMO gap is approximately the same in IQ and SQ but about a factor of two larger in HQ. These results correctly reproduce the trends seen in the more accurate, more computationally expensive time dependent density functional theory (TDDFT) calculations of Il'ichev and Simon [22]. This is consistent with the threshold for optical absorption found from semi-empirical methods [5, 20]. The large difference in the HOMO-LUMO gap between HQ and the other molecules may be important for “molecular engineering” applications and for explaining the broad band optical absorption of eumelanin. In particular, if the model of the eumelanins as amorphous semiconductors is correct it may allow the chemical tuning of the semiconducting band gap (c.f. Ref. [18]).

	IQ	SQ	HQ
TDDFT (PBE/B3LYP) [22]	1.82	1.50	4.53
TDDFT (B3LYP) [22]	1.79	1.43	4.30
NRLMOL (Δ SCF/PBE)	2.02	1.12	3.61
NRLMOL (PBE)	1.07	0.80	3.48
Hückel [17]	1.3	0.84	3.4

the values predicted by the two different methods as it is extremely unlikely that either method is incorrect by a large enough margin to allow the other to be correct.

The calculated Δ SCF HOMO-LUMO gap is also consistent with previously published semiempirical ZINDO (Zerner’s intermediate neglect of differential overlap) calculations of the optical absorption spectra [5, 20]. In particular Bolívar-Marinez *et al.* noted that “in the neutral state the threshold for optical absorption is around 2.0 eV for the IQ and SQ, while in the case of the HQ it is roughly 3.8 eV.” Taking these numbers as semiempirical estimates of the HOMO-LUMO gap they are in excellent agreement with our Δ SCF calculations (c.f. table III).

It is also interesting to note that the change in the SQ conformation observed in the calculations for the SQ + 6H₂O system caused a 7% decrease in Δ_{HL} relative to SQ in vacuo. It is possible that in a polar solvent a range of conformations exist which may lead to a broadening of the optical absorption [39].

In terms of Hückel theory, the difference between Δ_{HL} for HQ and IQ/SQ can be understood in terms of the level of delocalisation of the HOMOs and LUMOs. It should be noted that the aromatic ring in HQ contains

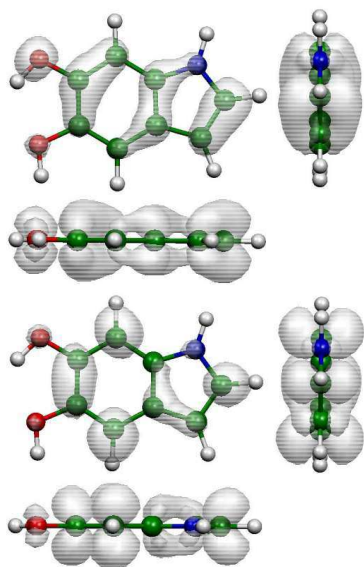


FIG. 2: The electron density in the highest occupied molecular orbital (HOMO) (top) and the lowest unoccupied molecular orbital LUMO (bottom) of hydroquinone (HQ). The atoms are colour coded as follows: carbon - green, nitrogen - blue, oxygen - red and hydrogen - white. The LUMO electron density is in good agreement with the semiempirical calculations of Bolívar-Marinez *et al.* [20], however there is some discrepancy in the HOMO electron density.

a resonating valence bond, whereas this feature is absent in IQ and SQ. This can be contrasted with the Hückel model result for benzene which predicts $\Delta_{\text{HL}} = 2\beta$ for the neutral molecule but if one double bond in the ring is replaced by a single bond, as in, for example, the reduced form C_6H_8 , then $\Delta_{\text{HL}} = 0$. On this basis one might well expect the HOMO-LUMO gap of HQ to be significantly larger than those of IQ and SQ. However, detailed plots of the electron densities in the HOMO and LUMO of the three molecules (figures 2, 3 and 4) indicate that the real situation is somewhat more complicated. The electron densities are significantly more localised in the HOMOs of IQ and SQ than the electron density of the HOMO of HQ is. In particular, the electron densities in the HOMOs and LUMOs of IQ and SQ are not as similar as one might expect from figure 1. However, even in the ΔSCF calculation, the HOMO-LUMO gap is a factor of two larger in HQ than it is in SQ and IQ.

In the absence of knowledge of the chemical structure of the eumelanins it is difficult to predict how a change in the HOMO-LUMO gap of the monomer will effect the electronic structure. However it is likely that changing Δ_{HL} by a factor of two will have a dramatic effect on the electronic structure of the melanin macromolecule. For example, it is reasonable to expect that the HOMO-LUMO gap of a macromolecule will be related to Δ_{HL} (c.f. Ref. [18]). Thus we expect that the HOMO-LUMO gap for a macromolecule of HQ will be significantly larger than that of a macromolecule of IQ or SQ. For a macro-

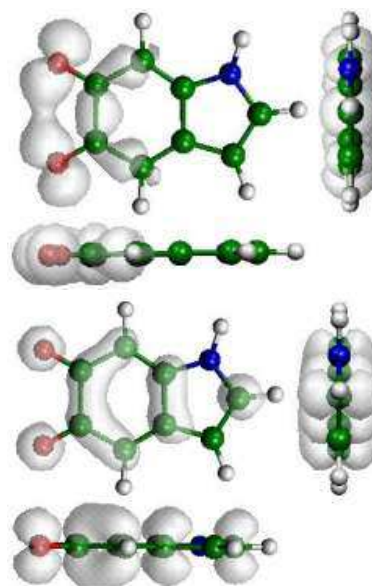


FIG. 3: The electron density in the highest occupied molecular orbital (HOMO) (top) and the lowest unoccupied molecular orbital LUMO (bottom) of indolequinone (IQ). The atoms are colour coded as follows: carbon - green, nitrogen - blue, oxygen - red and hydrogen - white. The LUMO electron density is in good agreement with the semiempirical calculations of Bolívar-Marinez *et al.* [20], however there is some discrepancy in the HOMO electron density.

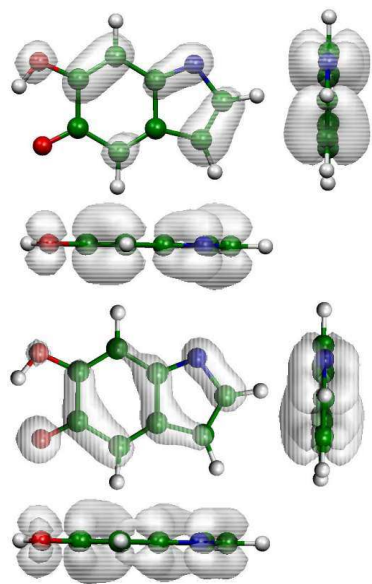


FIG. 4: The electron density in the highest occupied molecular orbital (HOMO) (top) and the lowest unoccupied molecular orbital LUMO (bottom) of semiquinone (SQ). The atoms are colour coded as follows: carbon - green, nitrogen - blue, oxygen - red and hydrogen - white. Both the HOMO and LUMO electron densities are in good agreement with the semiempirical calculations of Bolívar-Marinez *et al.* [20].

TABLE IV: The predicted Phonon (IR) and Raman spectra for hydroquinone (HQ).

Frequency (cm^{-1})	IR intensity ($\text{D}^2/\text{amu}\text{\AA}^2$)	Isotropic Raman scattering activity ($\text{\AA}^4/\text{amu}$)	Total Raman scattering activity ($\text{\AA}^4/\text{amu}$)
137.4	0.008	0.000	0.668
144.0	0.162	0.000	0.605
289.5	0.357	0.000	0.729
300.7	0.389	0.022	0.908
302.9	1.848	0.000	2.430
311.7	0.976	0.000	1.205
314.0	0.019	0.023	0.533
344.3	0.932	0.000	0.040
366.5	1.360	0.000	0.993
416.0	0.145	0.000	0.990
428.2	0.120	0.013	3.523
463.2	0.032	9.290	14.050
589.6	0.040	0.000	0.380
608.8	0.561	0.000	1.277
665.2	0.581	0.000	0.520
677.4	0.376	0.000	0.626
706.8	0.689	0.000	0.811
735.0	0.011	31.978	36.825
753.5	0.036	0.178	1.655
762.5	0.250	0.000	0.181
792.1	0.506	0.000	0.947
806.4	0.436	0.000	0.776
843.0	0.639	0.477	0.636
890.6	0.125	2.517	4.183
1055.2	0.291	21.980	28.451
1069.8	0.129	0.213	2.528
1104.2	2.271	1.698	2.285
1145.8	0.635	0.034	9.197
1159.9	8.026	0.708	1.406
1175.8	2.970	0.000	3.764
1217.1	0.303	1.202	2.299
1265.2	0.391	5.638	8.478
1328.6	0.909	26.707	45.852
1334.9	1.440	3.164	4.150
1360.6	0.213	68.155	122.963
1425.4	0.135	1.951	12.385
1462.3	2.384	3.954	38.040
1489.8	0.324	0.016	0.614
1511.3	1.122	64.105	92.156
1593.6	0.436	0.005	1.408
1628.4	0.366	3.559	21.170
3086.8	0.425	30.403	58.297
3090.6	0.257	90.643	170.535
3170.7	0.047	2.066	86.139
3189.4	0.033	128.345	185.587
3598.1	1.359	78.683	135.123
3709.9	1.153	74.758	126.550
3716.9	1.182	98.150	155.123

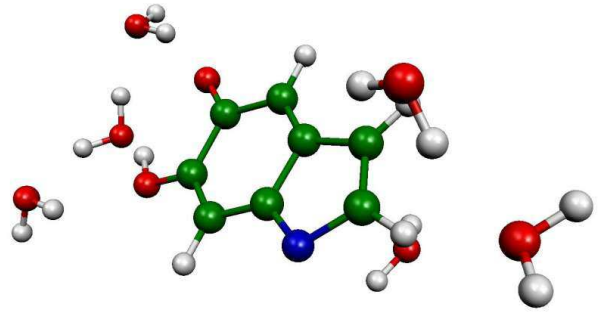


FIG. 5: The stable structure of semiquinone (SQ) and 6 H_2O molecules. Note the hydrogen bonded networks around the H-O-C-C=O group, which is dragged slightly out of the plan by the interactions with the solvent. The H-O-C bond angle has increased relative to that of the SQ molecule in vacuo.

molecule containing both HQ and, say, IQ this change in the electronic structure will act as a source of disorder and thus have a dramatic effect on the electronic transport properties.

It is also difficult, without detailed knowledge of the chemical structure of the eumelanins, to predict exactly how the variation of Δ_{HL} affects the optical absorption. However, it seems possible that the range of Δ_{HL} between different molecules may produce the continuum of HOMO-LUMO gaps in eumelanin macromolecules and thus play an important role in explaining the observed the broad band optical absorption.

It is therefore important to be able to identify the monomeric content of a sample of eumelanin, ideally this should be done *in situ* and non-destructively. Motivated by this fact we have calculated both the Raman and infrared (IR) spectra of IQ, SQ and HQ, (see tables IV, V and VI). This has several uses. Firstly, the prediction allows for experimental testing of the accuracy of our calculations. Secondly, it can be seen that there are notable differences in both the Raman and IR spectra of the three monomers (see, for example, figures 6 and 7). The Raman and IR spectra could therefore be used for the *in situ*, non-destructive identification of the monomeric content of macromolecules. This could be particularly valuable in the engineering of devices from eumelanins, as, by varying the ratio of indole-quinones, it may be possible to achieve control of the band-gap of the material. This may also be a useful analytical tool for the analysis of the structure of both synthetic and naturally occurring melanin, and thus be helpful in determining the structure-property-function relationships that control their behaviour.

Comparison of our calculated IR and Raman spectra with standard tables for organic molecules [40, 41] shows that the calculated phonon spectra are in broad agreement with known IR absorption band values (see table VII). It can also be seen from table VII that the differences in the spectra, specifically which vibrations are absent for a given molecule can be understood in terms

TABLE V: The predicted Phonon (IR) and Raman spectra for indolequinone (IQ).

Frequency (cm^{-1})	IR intensity ($\text{D}^2/\text{amu}\text{\AA}^2$)	Isotropic Raman scattering activity ($\text{\AA}^4/\text{amu}$)	Total Raman scattering activity ($\text{\AA}^4/\text{amu}$)
55.0	0.004	0.000	0.612
122.2	0.000	0.000	0.580
197.4	0.292	0.000	1.234
289.1	1.546	0.000	0.095
329.2	0.026	0.161	1.736
336.2	0.045	0.963	1.476
357.9	0.152	0.000	0.251
396.5	0.178	1.587	19.222
445.9	0.002	0.000	0.249
448.8	0.007	7.783	14.949
568.5	0.143	0.000	0.531
614.5	0.008	15.800	20.336
643.6	0.515	0.994	14.159
692.8	0.409	0.000	0.493
735.5	0.175	0.000	0.209
743.0	0.246	0.000	0.332
746.1	0.069	1.722	14.246
806.9	1.552	0.000	1.162
814.5	0.049	4.421	8.129
850.4	0.118	0.000	0.640
850.7	0.260	0.001	1.761
869.6	0.012	0.000	1.615
1047.0	1.402	1.668	17.404
1072.1	0.549	25.395	72.312
1104.1	0.006	10.970	38.889
1133.4	0.339	0.008	6.465
1184.8	0.119	2.879	6.366
1208.0	1.243	23.620	33.118
1218.5	1.682	0.037	0.926
1324.5	0.322	19.383	44.473
1343.5	4.097	0.757	25.939
1405.0	0.710	0.017	5.047
1533.9	1.998	125.526	209.070
1575.3	4.151	148.528	208.833
1623.9	2.864	8.682	131.748
1640.5	4.173	25.925	103.570
1667.0	0.874	0.699	17.584
3109.9	0.078	72.246	127.495
3121.8	0.040	90.847	166.066
3177.1	0.017	4.399	100.595
3195.5	0.003	133.664	192.718
3594.6	1.840	95.806	150.728

TABLE VI: The predicted Phonon (IR) and Raman spectra for semiquinone (SQ).

Frequency (cm^{-1})	IR intensity ($\text{D}^2/\text{amu}\text{\AA}^2$)	Isotropic Raman scattering activity ($\text{\AA}^4/\text{amu}$)	Total Raman scattering activity ($\text{\AA}^4/\text{amu}$)
89.5	0.161	0.000	0.573
136.3	0.004	0.000	0.242
221.8	0.001	0.000	0.318
307.7	0.164	1.094	1.619
348.8	0.034	0.023	0.434
352.9	0.025	0.000	0.121
383.3	0.461	0.000	0.080
402.1	0.041	0.057	0.561
447.6	0.069	11.923	25.667
458.3	2.024	0.000	1.902
516.1	0.000	0.000	1.370
628.7	0.770	2.541	5.507
656.8	0.077	15.330	22.320
686.7	0.337	0.000	0.263
748.5	0.034	0.000	0.697
753.8	0.051	3.268	4.895
756.0	0.322	0.000	0.476
813.9	0.045	0.071	1.579
820.4	0.121	2.587	8.251
833.0	0.422	0.000	1.924
885.4	0.849	0.000	0.653
902.3	0.053	0.000	1.303
983.0	0.542	5.903	87.829
1075.3	1.431	12.652	24.493
1087.2	2.371	13.610	22.939
1117.7	1.632	0.159	9.469
1173.4	0.801	0.135	2.521
1199.1	2.031	10.995	15.634
1233.3	1.360	0.819	4.704
1294.0	0.974	13.021	66.258
1356.8	0.767	2.578	8.707
1384.4	0.077	24.950	39.103
1499.3	0.607	248.871	433.636
1537.7	0.176	18.043	69.559
1585.3	4.588	70.696	147.517
1648.9	0.164	136.594	232.764
1650.3	5.288	26.421	93.212
3088.1	0.261	76.797	140.364
3121.5	0.026	60.571	122.056
3153.0	0.214	32.031	134.793
3181.5	0.076	123.921	185.037
3680.9	2.011	108.125	198.914

of their structure, c.f. figure 1, as expected.

It is important to stress that our calculated IR and Raman spectra are for gaseous phase monomers. Thus, the comparison of such results with experiment may be complicated by several factors. Firstly the formation of macromolecules may result in a significant change in the spectra. However, it is known that in other biomolecules the effect of polymerisation only slightly broadens the IR and Raman spectra, for example the spectra of simple amino acids is only slightly broadened in proteins [42]. Secondly solvent effects may largely ‘wash out’ the

individual features of the spectra [39, 43]. It is clear from our study of the SQ + 6H₂O system that there will be significant hydrogen bonding in the solvent, hydrogen bonding can shift the phonon frequencies [3]. Therefore it remains to be seen if, experimentally, the resolution is good enough to resolve the differences in the spectra of the monomers. However, an obvious way to avoid solvent effects is to conduct the experiments in the solid state.

TABLE VII: Broad assignments of the strongest bands in the simulated phonon (IR) spectra of HQ, SQ and IQ (FIG.6). The band assignments were made according to standard tables [40, 41].

Band (cm ⁻¹)	Group/Vibration	HQ	SQ	IQ
~1100	ν (C-OH) strong	present	present	absent
~1340	ν (Aromatic C-N) strong	present	absent	present
~1450-1590	ν (Aromatic C-C) strong	present	present	present
~1620-1650	ν (quinone C=O) strong	absent	present	present
~3590-3600	ν (N-H) medium	present	absent	present
~3700	ν (O-H) strong	present	present	absent

IV. CONCLUSIONS

We have carried out first principles density functional calculations for the hydroquinone (HQ), the indolequinone (IQ) and the semiquinone (SQ). The calculated gaseous phase structure is in good agreement with previous calculations. We have used the Δ SCF method to study the HOMO-LUMO gap. Our results are consistent with the threshold for optical absorption found by semiempirical methods. Specifically, we found that the HOMO-LUMO gap is similar in IQ and SQ but approximately twice as large in HQ. The possibility of using this difference in the HOMO-LUMO gap to engineer the electronic properties of eumelanins at the molecular level has been discussed. We have also suggested that the difference in the HOMO-LUMO gap of the different monomers could lead to a large range of HOMO-LUMO gaps in eumelanin macromolecules and thus be related to the observed broad band optical absorption.

As the structure of macromolecules of these monomers is not known we have also calculated the IR and Raman spectra of the three monomers from first principles. A comparison of these results with experiment would represent a stringent test of the density functional calculations as these calculations do not rely on additional semiempirical information. It was shown that the IR and Raman

spectra have potential as a analytical tool for these materials. Each of the monomers have significantly different spectral signatures, therefore the IR or Raman spectra could be used *in situ* to non-destructively investigate the monomeric content of macromolecules. It is hoped that this may be helpful in determining the structure of both natural and synthetic eumelanins, and hence aid our attempts to understand their biological functionality.

Acknowledgements

We would like to thank John Dobson, Joel Gilmore, Peter Innis, Urban Lundin, Jeffrey Reimers, Jennifer Riesz Cathy Stampfl and Linh Tran for helpful discussions. The work at the University of Queensland was supported by the Australian Research Council. BJP was supported in part by US Navy Grant N00014-03-1-4115. KB was supported in part by US Navy Grant N00014-03-1-4116. TB was supported in part by US Navy Grant N00014-02-1-1046. MRP was supported in part by ONR and the DoD HPC CHSSI initiative. BJP, RHM and MRP appreciate the hospitality of the Kavli Institute of Theoretical Physics, where this work was initiated. The KITP is supported by NSF through grant PHY99-07949.

-
- [1] G. Prota, *Melanins and Melanogenesis* (Academic Press, New York, 1992).
- [2] M. L. Wolbarsht, A. W. Walsh, and G. George, *Appl. Opt.* **20**, 2184 (1981).
- [3] K. E. van Holde, W. C. Johnson, and P. S. Ho, *Principles of Physical Biochemistry* (Prentice-Hall, Englewood Cliffs, NJ, 1998).
- [4] H. Z. Hill, *Melanin: Its Role in Human Photoprotection* (Valdenmar Press, Overland Park, KS, 1995).
- [5] K. B. Stark, J. M. Gallas, G. W. Zajac, and J. T. Golab, *J. Phys. Chem. B* **107**, 3061 (2003).
- [6] S. Ito, *Biophys. Acta* **883**, 155 (1986).
- [7] Z. W. Zajac, J. M. Gallas, J. Cheng, M. Eisner, S. C. Moss, and A. E. Alvarado-Swaisgood, *Biochim. Biophys. Acta* **1199**, 271 (1994).
- [8] C. M. R. Clancy, J. B. Nofsinger, R. K. Hanks, and J. D. Simon, *J. Chem. Phys. B* **104**, 7871 (2000).
- [9] H. C. Longuet-Higgins, *Arch. Biochem. Biophys.* **88**, 231 (1960).
- [10] A. Pullman and B. Pullman, *Biochim. Biophys. Acta* **54**, 384 (1961).
- [11] J. McGinness, J. P. Corry, and P. Proctor, *Science* **183**, 853 (1974).
- [12] N. F. Mott and E. A. Davis, *Electronic Processes in Non-Crystalline Materials* (Clarendon Press, Oxford, 1971).
- [13] P. R. Crippa, V. Cristofolletti, and N. Romeo, *Biochim. Biophys. Acta* **538**, 164 (1978).
- [14] M. M. Jastrzebska, V. Cristofolletti, and N. Romeo, *Biochim. Biophys. Acta* **7**, 781 (1996).
- [15] P. Meredith and J. Riesz, cond-mat/0312277 (to appear in *Photochem. Photobiol.*).
- [16] J. Riesz, Honours thesis, University of Queensland (2003).
- [17] D. S. Galvão and M. J. Caldas, *J. Chem. Phys.* **88**, 4088 (1988).
- [18] D. S. Galvão and M. J. Caldas, *J. Chem. Phys.* **92**, 2630 (1990).

- [19] D. S. Galvão and M. J. Caldas, *J. Chem. Phys.* **93**, 2848 (1990).
- [20] L. E. Bolívar-Marinez, D. S. Galvão, and M. J. Caldas, *J. Phys. Chem. B* **103**, 2993 (1999).
- [21] K. Bochenek and E. Gudowska-Nowak, *Chem. Phys. Lett.* **373**, 523 (2003).
- [22] Y. V. Il'ichev and J. D. Simon, *J. Phys. Chem. B* **107**, 7162 (2003).
- [23] C. Lambert, J. N. Chacon, M. R. Chedekel, E. J. Land, P. A. Riley, A. Thonpson, and T. G. Truscott, *Biochem. Biophys. Acta* **993**, 12 (1989).
- [24] C. Lambert, E. J. Land, P. A. Riley, and T. G. Truscott, *Biochem. Biophys. Acta* **1035**, 319 (1990).
- [25] A. T. Al-Kazwini, P. O'Neill, G. E. Adams, R. B. Cundall, B. Jacquet, G. Lang, and A. Junino, *J. Phys. Chem.* **94**, 6666 (1990).
- [26] A. T. Al-Kazwini, P. O'Neill, G. E. Adams, R. B. Cundall, G. Lang, and A. Junino, *J. Chem. Soc., Perkin Trans. 2* **12**, 1941 (1991).
- [27] A. T. Al-Kazwini, P. O'Neill, R. B. Cundall, G. E. Adams, A. Junino, and J. Maignan, *Tetrahedron Lett.* **33**, 3045 (1992).
- [28] A. T. Al-Kazwini, P. O'Neill, G. E. Adams, R. B. Cundall, A. Junino, and J. Maignan, *J. Chem. Soc., Perkin Trans. 2* **13**, 657 (1992).
- [29] M. R. Pederson and K. A. Jackson, *Phys. Rev. B* **41**, 7453 (1990).
- [30] K. A. Jackson and M. R. Pederson, *Phys. Rev. B* **42**, 3276 (1990).
- [31] M. R. Pederson and K. A. Jackson, *Phys. Rev. B* **43**, 7312 (1991).
- [32] A. A. Quong, M. R. Pederson, and J. L. Feldman, *Solid State Commun.* **87**, 535 (1993).
- [33] D. V. Porezag and M. R. Pederson, *Phys. Rev. B* **54**, 7830 (1996).
- [34] D. V. Porezag, Ph.D. thesis, Technische Universität (1997), <http://archiv.tu-chemnitz.de/pub/1997/0025>.
- [35] A. Briley, M. R. Pederson, K. A. Jackson, D. C. Patton, and D. V. Porezag, *Phys. Rev. B* **58**, 1786 (1998).
- [36] J. P. Perdew, K. Burke, and M. Ernzerhof, *Phys. Rev. Lett.* **77**, 3865 (1996).
- [37] J. P. Lowe, *Quantum Chemistry* (Academic Press, London, 1978).
- [38] R. O. Jones and O. Gunnarsson, *Rev. Mod. Phys.* **61**, 689 (1989).
- [39] A. B. Myers, *Ann. Rev. Phys. Chem.* **49**, 267 (1998).
- [40] K. Nakanishi and P. H. Solomon, *Infrared Absorption Spectroscopy* (Holden-Day Inc., San Francisco, 1977).
- [41] E. B. Schrader, *Infrared and Raman Spectroscopy, Methods and Applications* (VCH Publishers, New York, 1995).
- [42] A. Xie, L. van der Meer, W. Hoff, and R. H. Austin, *Phys. Rev. Lett.* **84**, 5345 (2000).
- [43] C. Reichardt, *Solvents and Solvent Effects in Organic Chemistry* (VCH Verlagsgesellschaft, Basel, 1998).
-

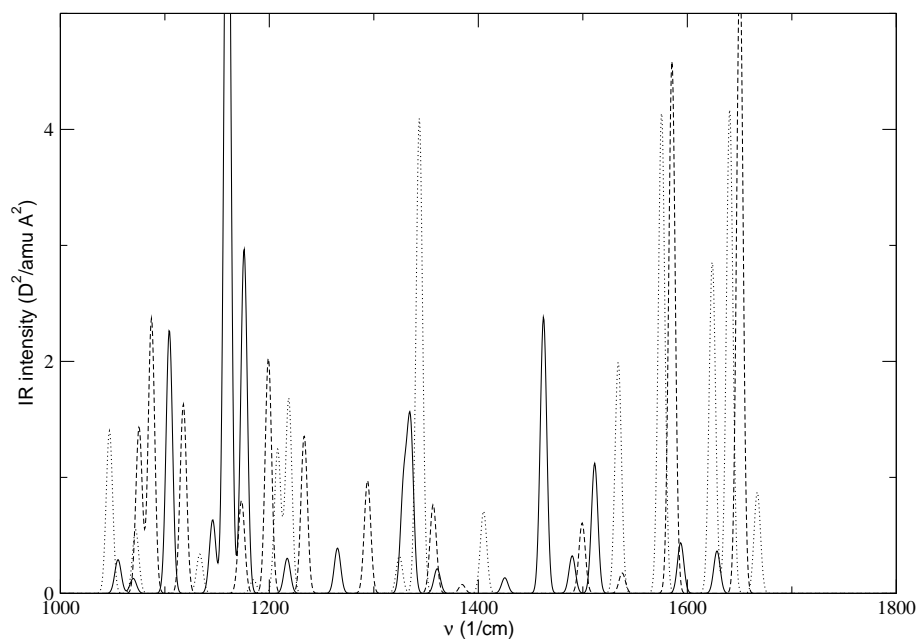


FIG. 6: Detail of the phonon (IR) spectra of hydroquinone (HQ) (solid line), semiquinone (SQ) (dashed line) and indolequinone (IQ) (dotted line). Clear differences can be seen between the spectra of the three monomers. For example, there are strong features around 1100cm^{-1} in both HQ and SQ but not in IQ. On the other hand, there are strong bands between ~ 1620 and 1650cm^{-1} in SQ and IQ which are absent in HQ (for broad assignments see table VII). This confirms that the IR spectra could be useful as in situ, non-destructive probes for identifying the monomeric content of eumelanins. To allow us to plot the spectra and to aid comparison with experiment we have broadened each peak by 6cm^{-1} , a value that is comparable to that seen experimentally for other biomolecules in solution [3].

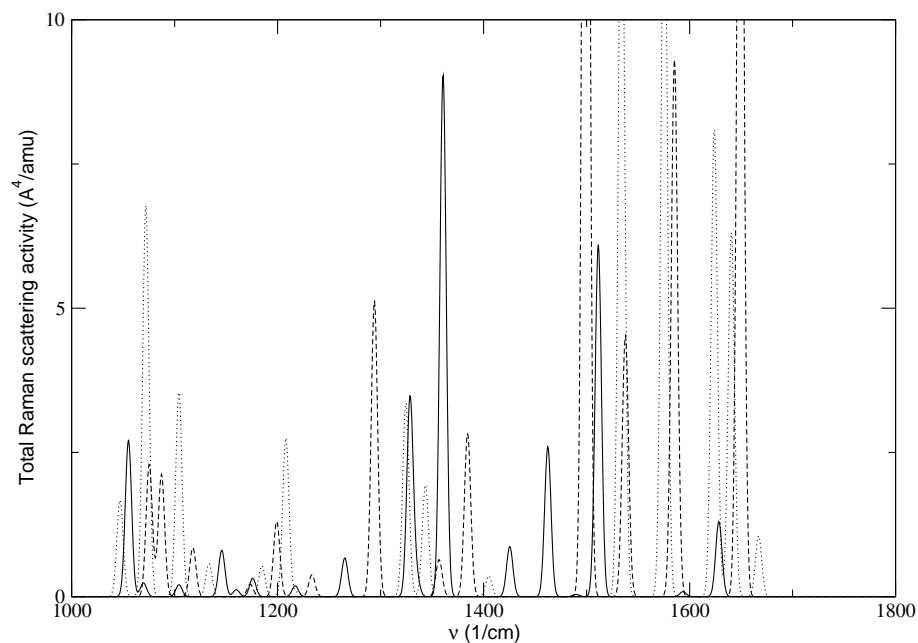


FIG. 7: Detail of the Raman spectra of hydroquinone (HQ) (solid line), semiquinone (SQ) (dashed line) and indolequinone (IQ) (dotted line). Once again, there are clear differences between the spectra of the three monomers confirming that Raman spectra could be useful as in situ, non-destructive probes for identifying the monomeric content of eumelanins. To allow us to plot the spectra and to aid comparison with experiment we have broadened each peak by 6cm^{-1} , a value that is comparable to that seen experimentally for other biomolecules in solution [3].